

DTIC FILE COPY

AD _____



MODELING OF THE NON-AUDITORY RESPONSE TO BLAST OVERPRESSURE

AD-A223 393

A Surrogate Model of
Thoracic Response to Blast Loading

ANNUAL/FINAL REPORT

J. H.-Y. Yu
H. H. Ho
J. H. Stuhmiller

JANUARY 1990

DTIC
ELECTE
JUL 02 1990
S D
GE

Supported by

U.S. ARMY MEDICAL RESEARCH AND DEVELOPMENT COMMAND
Fort Detrick, Frederick, Maryland 21701-5012

Contract No. DAMD17-85-C-5238

JAYCOR
11011 Torreyana Road
San Diego, California 92121-1190

Approved for public release; distribution unlimited

The findings in this report are not to be construed as an
official Department of the Army position unless so
designated by other authorized documents.

90 07 2 039

MODELING OF THE NON-AUDITORY RESPONSE TO BLAST OVERPRESSURE

A Surrogate Model of Thoracic Response to Blast Loading

JANUARY 1990

Supported by

**U.S. ARMY MEDICAL RESEARCH
AND DEVELOPMENT COMMAND**

**Fort Detrick
Frederick, Maryland 21701-5012**

Contract No. DAMD17-85-C-5238

Accession For	
NTIS GRA&I	<input checked="" type="checkbox"/>
DTIC TAB	<input type="checkbox"/>
Unannounced	<input type="checkbox"/>
Justification	
By _____	
Distribution/	
Availability Codes	
Dist	Avail and/or Special
A-1	



REPORT DOCUMENTATION PAGE

1a. REPORT SECURITY CLASSIFICATION Unclassified		1b. RESTRICTIVE MARKINGS N/A	
2a. SECURITY CLASSIFICATION AUTHORITY N/A		3. DISTRIBUTION / AVAILABILITY OF REPORT Approved for Public Release; Distribution unlimited	
2b. DECLASSIFICATION / DOWNGRADING SCHEDULE N/A			
4. PERFORMING ORGANIZATION REPORT NUMBER(S)		5. MONITORING ORGANIZATION REPORT NUMBER(S)	
6a. NAME OF PERFORMING ORGANIZATION JAYCOR Applied Sci. & Engr. Technol. Group	6b. OFFICE SYMBOL (If applicable)	7a. NAME OF MONITORING ORGANIZATION Director Walter Reed Army Institute of Research	
6c. ADDRESS (City, State, and ZIP Code) 11011 Torreyana Rd. San Diego, CA 92121-1190		7b. ADDRESS (City, State, and ZIP Code) ATTN: SGRD-UWZ-C, Kenneth T. Dodd, Ph.D. Bldg. 40 Washington, DC 20307-5100	
8a. NAME OF FUNDING / SPONSORING ORGANIZATION U. S. Army Medical Res. & Devel. Cmd.	8b. OFFICE SYMBOL (If applicable)	9. PROCUREMENT INSTRUMENT IDENTIFICATION NUMBER DAMD17-85-C-5238	
8c. ADDRESS (City, State, and ZIP Code) Fort Detrick Frederick, MD 21701-5012		1c. SOURCE OF FUNDING NUMBERS	
		PROGRAM ELEMENT NO. 62787A	PROJECT NO. 62787A878
		TASK NO. AB	WORK UNIT ACCESSION NO. 004
11. TITLE (Include Security Classification) (U) Modeling of the Non-Auditory Response to Blast Overpressure			
12. PERSONAL AUTHOR(S) J. H.-Y. Yu, H. H. Ho, and J. H. Stuhmiller			
13a. TYPE OF REPORT Annual/Final	13b. TIME COVERED FROM 8/15/85 TO 7/31/89	14. DATE OF REPORT (Year, Month, Day) 1990 January	15. PAGE COUNT 50
16. SUPPLEMENTARY NOTATION \Rightarrow meters per second A Surrogate Model of Thoracic Response to Blast Loading			
17. COSATI CODES		18. SUBJECT TERMS (Continue on reverse if necessary and identify by block number)	
FIELD	GROUP	SUB-GROUP	
26	14	RA3, Surrogate model of thoracic response to blast loading, Explosions, Injury, ITP	
23	04	Intrathoracic pressure	
19. ABSTRACT (Continue on reverse if necessary and identify by block number) A surrogate material was sought to facilitate laboratory model tests on the dynamics of blast injury of the lung. Off-the-shelf shaving cream (foam) was found to have a nominal density of 0.1 g/cm ³ and a wave speed of 35 m/s similar to that of the lung parenchyma, and was chosen as the surrogate material. ^{0.1 gram per centimeter Cubed} Pressure measurements in a foam-filled tube indicate that a shock-like pressure wave develops in the foam under blast loading. This wave is dissipated and dispersed as it moves downstream. The shock-like characteristics are absent, however, when the pressure is measured in a small-diameter tubular balloon, or in the bronchial tube of a rabbit lung, placed in the foam. This result suggests that conventional intrathoracic pressure (ITP) measurements obtained in animal airways or the esophagus may not be representative of the true lung parenchymal pressure and could be misleading. A thoracic model that uses the surrogate lung material and a chest wall model was fabricated to test the applicability of the $p = \rho cv$ relationship. It was found that within the blast loading range tested, which produces accelerations of up to about 20,000 g and velocities of 11 m/sec, pressure signals up to their peaks agree well with ρcv . Limitations in instrument resolution, however, preclude the comparison beyond peak pressure.			
20. DISTRIBUTION / AVAILABILITY OF ABSTRACT <input type="checkbox"/> UNCLASSIFIED/UNLIMITED <input checked="" type="checkbox"/> SAME AS RPT. <input type="checkbox"/> DTIC USERS		21. ABSTRACT SECURITY CLASSIFICATION Unclassified	
22a. NAME OF RESPONSIBLE INDIVIDUAL Mary Frances Bostian		22b. TELEPHONE (Include Area Code) [301] 663-7325	22c. OFFICE SYMBOL SGRD-RM-S

13. ABSTRACT (Continued from front)

A SURROGATE MODEL OF THORACIC RESPONSE TO BLAST LOADING

**James H.-Y. Yu
Kevin H.-H. Ho
James H. Stuhmiller
Applied Science and Engineering Technology
JAYCOR**

ABSTRACT

A surrogate material was sought to facilitate laboratory model tests on the dynamics of blast injury of the lung. Off-the-shelf shaving cream (foam) was found to have a nominal density of 0.1 g/cm^3 and a wave speed of 35 m/s, similar to that of the lung parenchyma, and was chosen as the surrogate material.

Pressure measurements in a foam-filled tube indicate that a shock-like pressure wave develops in the foam under blast loading. This wave is dissipated and dispersed as it moves downstream.

The shock-like characteristics are absent, however, when the pressure is measured in a small-diameter tubular balloon, or in the bronchial tube of a rabbit lung, placed in the foam. This result suggests that conventional intrathoracic pressure (ITP) measurements obtained in animal airways or the esophagus may not be representative of the true lung parenchymal pressure and could be misleading.

A thoracic model that uses the surrogate lung material and a chest wall model was fabricated to test the applicability of the $p = \rho cv$ relationship. It was found that within the blast loading range tested, which produces accelerations of up to about 20,000 g and velocities of 11 m/sec, pressure signals up to their peaks agree well with ρcv . Limitations in instrument resolution, however, preclude the comparison beyond peak pressure.

CONTENTS

	<u>Page</u>
ABSTRACT	
1. INTRODUCTION	1-1
2. SURROGATE LUNG MATERIAL	2-1
2.1 Material Properties of an Animal Lung	2-1
2.2 Speed of Sound in a Gas-Liquid Mixture	2-1
2.3 The Surrogate Lung Material	2-6
2.3.1 Material Properties of the Surrogate Lung Material	2-6
2.3.2 Surrogate Lung Material Wave Property Tests	2-6
3. SURROGATE THORAX MODEL TESTS	3-1
4. APPLICATIONS OF THE SURROGATE MATERIAL AND THORAX MODEL	4-1
4.1 Pressure Dissipation in the Surrogate Material	4-1
4.2 Correlation Between Chest Wall Velocity and Parenchyma Pressure	4-1
4.3 Interpretation of Intrathoracic Pressure (ITP) Measurement	4-5
5. CONCLUSIONS	5-1
REFERENCES	R-1

ILLUSTRATIONS

<u>Figure</u>	<u>Page</u>
1. Intrathoracic pressure average of experimental data over all shots	2-3
2. Comparison of measured sound speed of two-phase materials with theory	2-5
3. Speed of sound versus density for air, water and various air/water organs and mixtures	2-7
4. Density variation of the shaving cream versus the dispense ratio from a pressurized container	2-8
5. Foam wave property test setup	2-9
6. Schematic diagram of surrogate thorax model test setup	3-2
7. Surrogate thorax model test setup	3-3
8. Chest wall model and instrumentation	3-4
9. Loading measurements across a 1-D chest wall model	3-5
10. Blast pressure variation in the foam at various stations along the test pipe	4-2
11. Pressure variation versus distance	4-3
12. Comparison of the measurement results of p and pcv at the 1-D foam-chest wall model interface	4-4
13a. High impulse chest wall model	4-6
13b. High impulse chest wall test model setup	4-7
14. Comparison of p vs. pcv for high impulse model test	4-8
15. Test setup for pressure measurements in air sack vs. in surrogate lung material	4-10
16. Pressure signal inside vs. outside of a tubular balloon	4-11

Figure	Page
17. Pressure signals inside a foam-filled balloon and in the surrounding foam	4-12
18. Pressure signal inside an air-filled balloon vs. a foam-filled balloon	4-14
19. Pressure signals in the bronchi, parenchyma, and surrogate lung material	4-15

TABLES

	<u>Page</u>
1. Density and Wave Speed in Lung	2-2

1. INTRODUCTION

Blast-induced lung injury has been the subject of research for many years. Empirical relationships on lung injury have been established in terms of animal body weight and loading characteristics (peak pressure, peak impulse) for certain blast conditions and animal orientations (Richmond, et al., 1968). Applicability of these relationships becomes questionable, however, when blast conditions are different from those of the original tests, such as in complex waves, for different species, different body geometry, or orientation.

To circumvent this deficiency, an understanding is needed of the dynamics connecting blast loading to parenchyma injury. Once the dynamics are fully understood and a corresponding injury threshold for the lung is established, predictive models of injury for both simple and complex waves and for various body geometries can be formulated.

Loading of the chest wall, stress wave propagation through the lung, and the mechanisms of injury need to be studied separately to gain a generalizable understanding of the injury process. In this report, we characterize the dynamics of loading and subsequent stress wave propagation in the lung by using a surrogate material. This approach allows us to avoid the use of test animals (which can be used separately to determine the injury mechanism) and provides a more convenient medium for controlled tests.

To represent the thorax dynamics realistically, the surrogate lung material must possess material properties similar to that of the lung parenchyma and the thorax model should have the same response characteristics as that of the chest wall. An appropriate material was identified and a mechanical thorax model constructed. Tests using this model have been used to establish the relationship between the chest wall motion and the pleural pressure, the dissipation rate of the pressure waves as it propagates through the lung, and the differences between pressure measurements made in the large airways and in the parenchyma itself.

2. SURROGATE LUNG MATERIAL

2.1 MATERIAL PROPERTIES OF AN ANIMAL LUNG

To capture the dynamics of the lung under blast loading, the density and wave speed of a surrogate material must be similar to those of the lung parenchyma.

The density of a lung depends on its degree of inflation. For an in vivo lung, the transpulmonary pressure is about 5 cm H₂O (Proctor et al., 1968; Agostoni et al., 1970). Furthermore, in order to inflate an excised lung to its in vivo condition, extra pressure is required to overcome the gravity effect. A reasonable pressurization range is about 5 to 10 cm H₂O (Selkurt, 1976). The lung density and wave speed corresponding to this pressure range for both rabbit and goat lungs, are on the order of 0.1 gm/cm³ and 35 m/s, respectively (Table 1).

The wave speed in live animals was estimated from field test data. Blast loading applied to the right side of the sheep induces a pressure pulse that starts at the right edge of the lung, passes through the right center, crosses into the left center, and finally reaches the left edge of the lung. A typical set of pressure signals measured at known transverse locations (determined from x-ray photographs) is shown in Figure 1. Though the results are masked by irregularities caused by body geometry and wave interaction complexities, the times of arrival of pressure peaks are distinct. An average wave speed of roughly 33 m/sec, similar to that derived from the isolated lung tests, is obtained.

2.2 SPEED OF SOUND IN A GAS-LIQUID MIXTURE

For an elastic continuum, the speed of sound (or stress wave) depends on its material density and modulus of elasticity. A similar functional relationship can be derived for a homogeneous two phase material. It was shown by Rice (1983) that when the composite modulus of elasticity and density of a two phase material were used, the wave speed, c , can be expressed as

$$c = (E/\rho)^{1/2} \quad (2-1)$$

where E is the modulus of elasticity of volume change and ρ is the mass density.

Let α and $(1 - \alpha)$ be the volumetric ratios of liquid and gas, respectively; then the composite modulus of elasticity of the medium (Rice, 1983) is

$$E = \frac{1}{\frac{1 - \alpha}{E_g} + \frac{\alpha}{E_l}} \quad (2-2)$$

where the subscripts g and l stand for gas and liquid (or tissue), respectively. The average density of the composite material is given by

Table 1. Density and Wave Speed in Lung.

Lung Tissue	Wave Speed (m/sec)	Density (g/cm ³)	PA - PPL (cm H ₂ O)	Reference
Horse (atelectatic)	25.0	0.60		Rice (1983)
Horse	30.2	0.29	0	Rice (1983)
	42.7	0.13	5	Rice (1983)
	60.4	0.09	20	Rice (1983)
Sheep	31.4-35.2			Field data
Goat	31.4		0	Yen et al. (1986)
	33.9		5	Yen et al. (1986)
	36.1		10	Yen et al. (1986)
	46.8		15	Yen et al. (1986)
	64.7		20	Yen et al. (1986)
Rabbit	16.5	0.60	0	Yen et al. (1986)
	28.9	0.15	4	Yen et al. (1986)
	31.3	0.12	8	Yen et al. (1986)
	35.3	0.11	12	Yen et al. (1986)
	36.9	0.10	16	Yen et al. (1986)

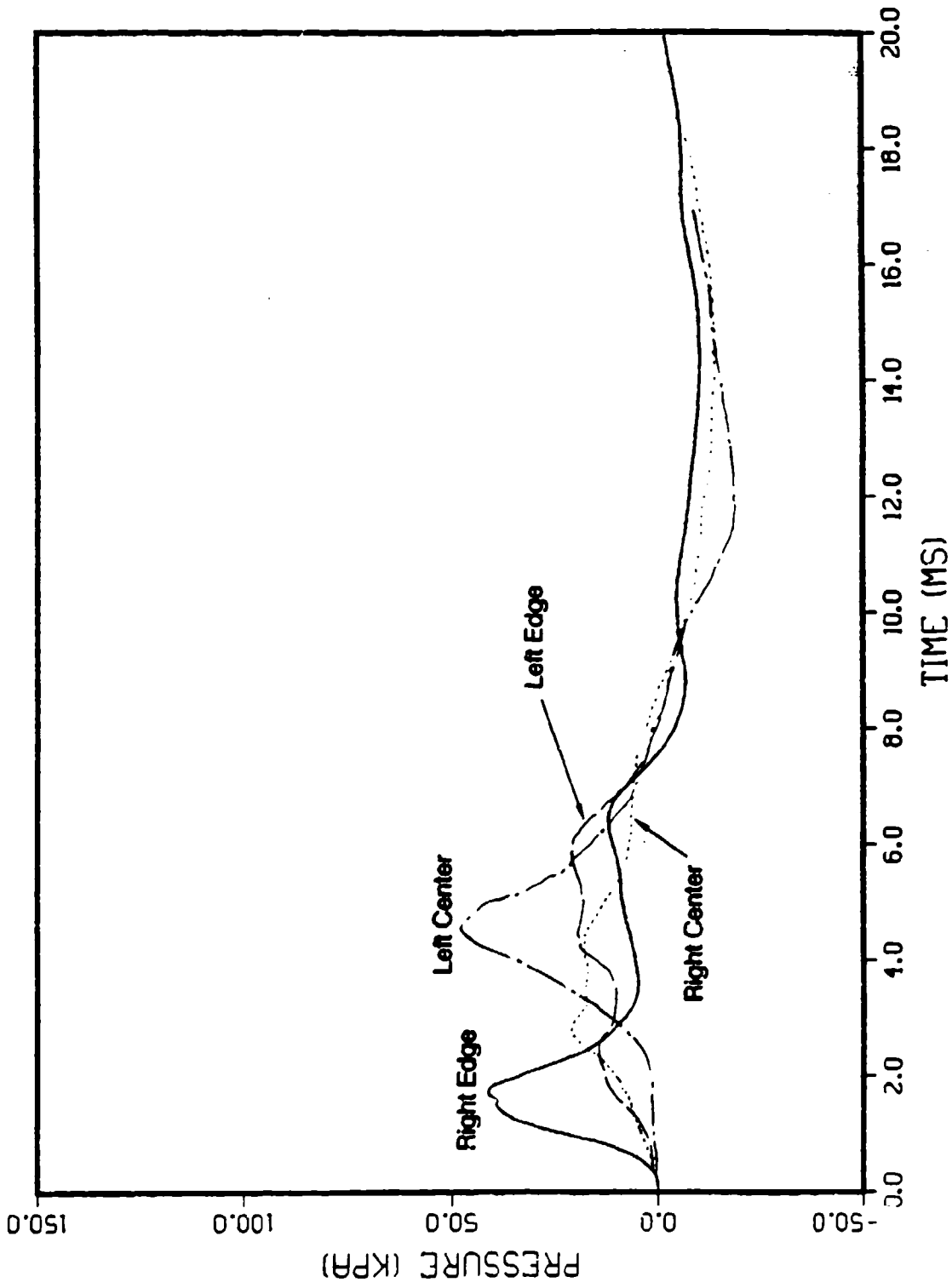


Figure 1. Intrathoracic pressure average of experimental data over all shots. Thoracic pressure, series 10, sheep D15.

$$\rho = (1 - \alpha)\rho_g + \alpha\rho_l \quad (2-3)$$

Since for all homogeneous materials

$$E = \rho(dp/d\rho) \quad ,$$

where p is the pressure, and for a perfect gas

$$p = \rho_g^\gamma \quad ,$$

therefore,

$$dp/d\rho_g = \gamma\rho_g^{(\gamma-1)} \quad ,$$

and

$$E_g = \gamma p \quad (2-4)$$

Substituting Eqs. (2), (3), and (4) into (1), we get

$$c = \left[\left(\frac{1 - \alpha}{\gamma p} + \frac{\alpha}{E_l} \right) \left((1 - \alpha)\rho_g + \alpha\rho_l \right) \right]^{-1/2} \quad (2-5)$$

At atmospheric conditions

$$\rho_g = 1.2 \times 10^{-3} \text{ g/cm}^3$$

$$\rho_l = 1 \text{ g/cm}^3$$

$$p = 100 \text{ kPa}$$

$$E_l = 2.20 \times 10^6 \text{ kPa}$$

Equation (2-5) is plotted in Figure 2 for $\gamma = 1.4$ (adiabatic processes) and $\gamma = 1.0$ (isothermal processes).

As shown, the speed of sound has a minimum value at about $\alpha = 0.5$. It then increases as the density either increases or decreases.

Since the lung tissue is essentially composed of water, the inflated lung can be regarded as an air-water two phase mixture. Figure 2 also includes the speed of sound measurements by Rice (1983) and Yen et al. (1986). In the normal lung density range (around 0.1 gm/cm^3), a higher density corresponds to a lower wave speed, and vice versa. The data obtained by the controlled tests of Yen et al. agrees well with the prediction, while that of Rice tends to systematically deviate

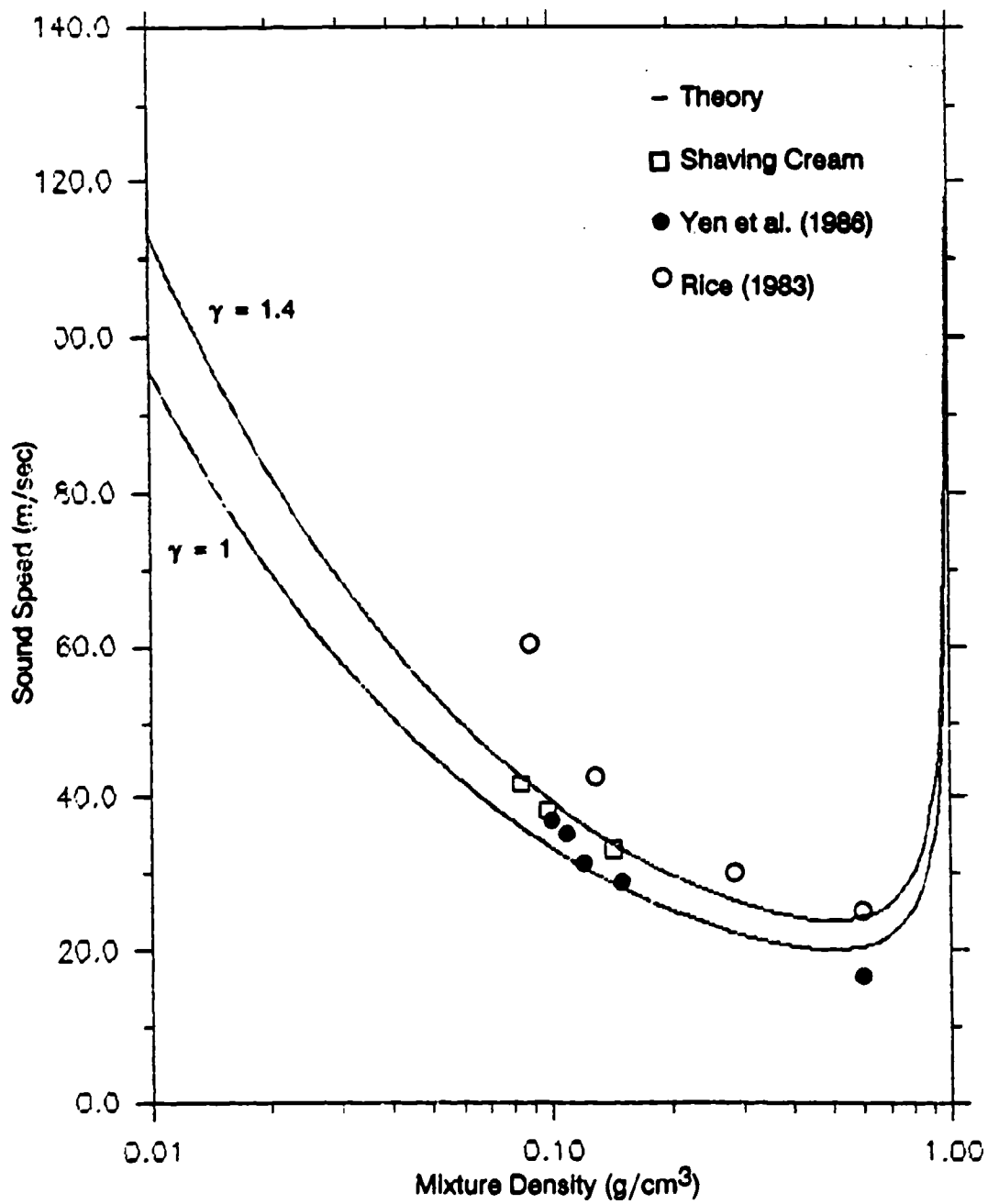


Figure 2. Comparison of measured sound speed of two-phase materials with theory.

from the theory. This is probably the result of uncertainty in density and/or wave speed measurements. The speeds of sound for air, water, and various two phase materials are compiled in Figure 3 to compare with the theory. As shown, the predicted wave speed agrees well with the data over the entire air-to-water density range.

2.3 THE SURROGATE LUNG MATERIAL

2.3.1 Material Properties of the Surrogate Lung Material

Since it is plausible that blast injury in lung is related to the propagation of stress waves through the lung, a realistic surrogate material should have the same wave characteristics as that of the lung parenchyma. Furthermore, since the wave speed depends on the material compressibility and density, we focus our material selection on those low density, two phase materials. We found that Colgate shaving cream dispensed from a pressurized container possessed such properties.

To determine the foam density, styrofoam cups were weighed and their volumes determined by measuring the amount of water required to fill them. The cups were filled with foam and weighed. The net weight for the known volume of foam determined the foam density.

Figure 4 shows the density variation of the foam versus the "consumption ratio" (the number of cups dispensed divided by the total number of cups available from a container) for two complete sets of tests. The density increases with the amount of foam dispensed and is especially pronounced near the end. Because of the higher initial pressure of the contents, the foam expands more when exposed and has a lower density. As more and more of the contents is dispensed, the pressure in the container decreases and the amount of expansion decreases, consequently the density increases. The bulk of the contents, say the middle 50 percent, however, varies only in a narrow density range of 0.095 to 0.10 gm/cc and matches well with that of an in vivo lung.

2.3.2 Surrogate Lung Material Wave Property Tests

The wave characteristics of the foam were measured in the prismatic Plexiglas test section ($5.08 \times 5.08 \times 17.8$ cm) shown in Figure 5. Blast loading was provided by the power loads of a Red Head Powder-Actuated-Tool (PAT) applied through a 10.2 cm diameter, 1 m long shock tube at the test surface. The blast was modified by a conditioning chamber at the muzzle of the PAT to provide a uniform target pressure distribution. The test section was isolated from the shock tube to reduce the "noise" of the blast signal and to prevent wave propagation through the apparatus by direct contact. Peak pressures of up to 70 kPa at the inlet were produced by using a No. 8w2 power load.

The blast pressure was coupled to the surrogate material via a closed-cell neoprene membrane. Pressure signals in the model were measured with two types of pressure transducers: Kistler wall-mounted transducers for side-on pressure measurements, and Millar Mikro-Tip transducers for pressure measurements within the foam. Wave speed of the foam was determined from pressure pulse travel time between two transducers a known distance apart.

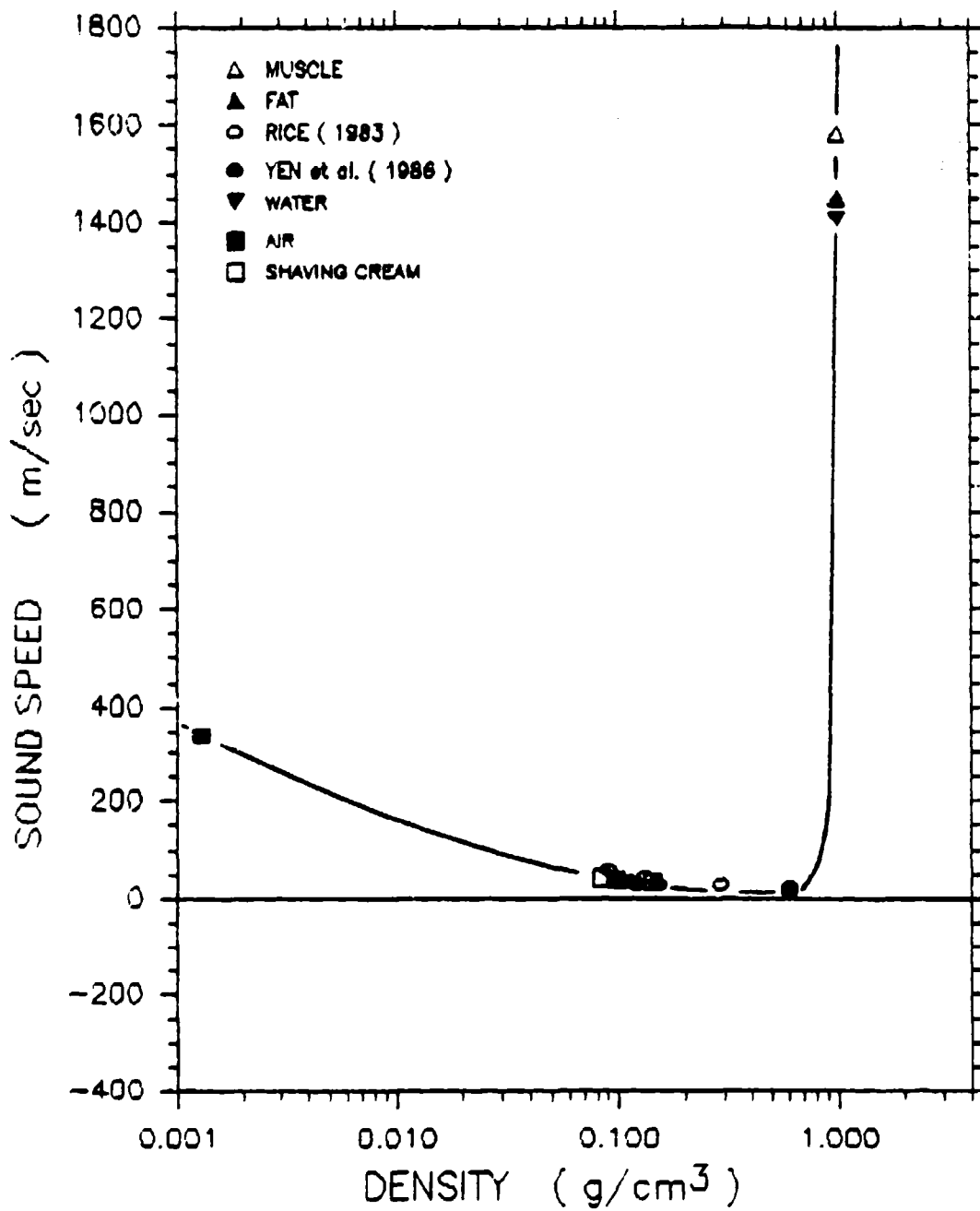


Figure 3. Speed of sound versus density for air, water and various air/water organs and mixtures.

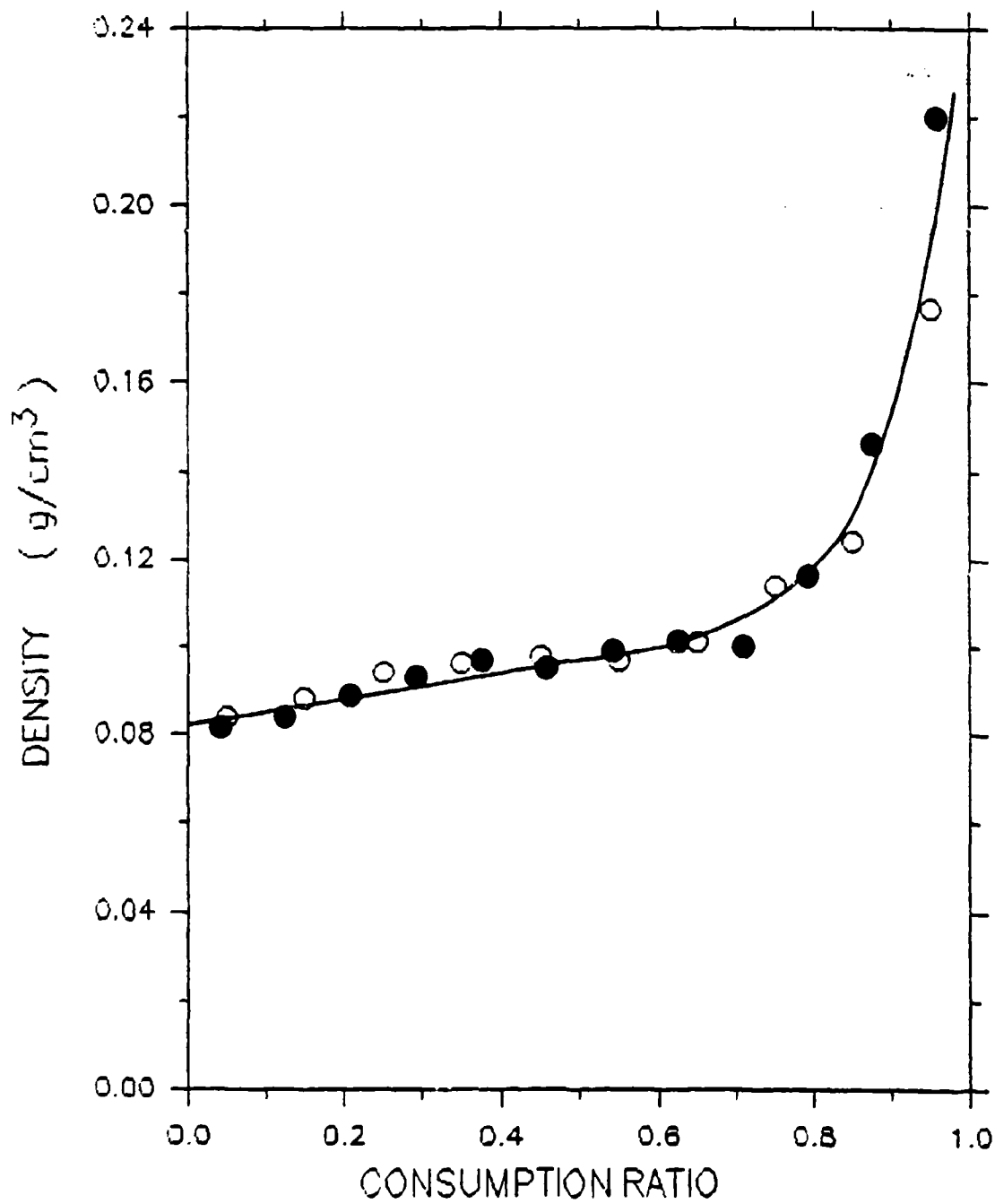


Figure 4. Density variation of the shaving cream versus the dispense ratio from a pressurized container.



Figure 5. Foam wave property test setup.

The wave speeds for different foam densities are also included in Figures 2 and 3. These values agree well with the theoretical prediction as well as the lung data of Yen, et al. and indicate that foam can be used to model the lung parenchyma.

3. SURROGATE THORAX MODEL TESTS

Blast loading applied to the chest wall of an animal produces a chest wall displacement that compresses the lung and sets up a stress wave. Depending on the amount of strain accompanying the stress wave, different degrees of injury may occur.

The net force per unit area on the chest wall is equal to the pressure difference between that on the front surface, p_1 , and that at the pleural surface, p_2 , neglecting any other support forces. This net force produces a corresponding chest wall acceleration, a , given by

$$(p_1 - p_2) = ma \quad (3-1)$$

where m is the chest wall mass per unit area.

A thorax model was constructed to duplicate this dynamic relation. The thorax model is made of Plexiglas and filled with foam. A free floating Plexiglas plate installed in front of the surrogate material is used as the model chest wall. A small shock tube is used to provide the blast loading. A schematic diagram of the model is shown in Figure 6, and a photograph of the test setup is shown in Figure 7.

The face-on blast loading on the model chest wall is measured by a forward-facing Kistler pressure transducer and the foam-side pressure is measured by a Millar Mikro-Tip transducer. Acceleration of the model is measured by a Kistler model 8616A low mass accelerometer. The instrumentation configuration of the model chest wall is shown in Figure 8. With instrumentation, the chest wall model has a mass density of 3.5 g/cm^2 .

The density of a sheep chest wall can be estimated as follows. Assume the sheep has a chest wall is 2.0 cm thick and the rib cage is 1 cm thick and covers one-half of the surface area. By using densities of 1 g/cm^3 for muscle and 2.0 g/cm^3 for bone (Fung, et al., 1985), we obtain an average chest wall density of 2.5 g/cm^2 , comparable to the Plexiglas model.

A typical set of low blast pressure test results is shown in Figure 9. INPUT stands for the reference pressure measured on the side-wall of the shock tube; FRONT and BACK represent the pressure outputs of the Kistler and the Millar pressure transducers, respectively; and ACCEL is the accelerometer output.

As shown, the FRONT pressure has the same general features as the acceleration signal: An instantaneous rise and short duration. The BACK pressure has a much lower amplitude, a second peak (caused by wave reflection), and a long duration. Because of the noisiness of these signals, it is difficult to compare directly the quantities in the force balance equation. Instead, we compare the impulse and momentum per unit area at each time step over the loading period. These quantities are found by integrating (3-1) with respect to time

$$\int_0^t (p_2 - p_1) dt = \int_0^t ma dt \quad (3-2)$$

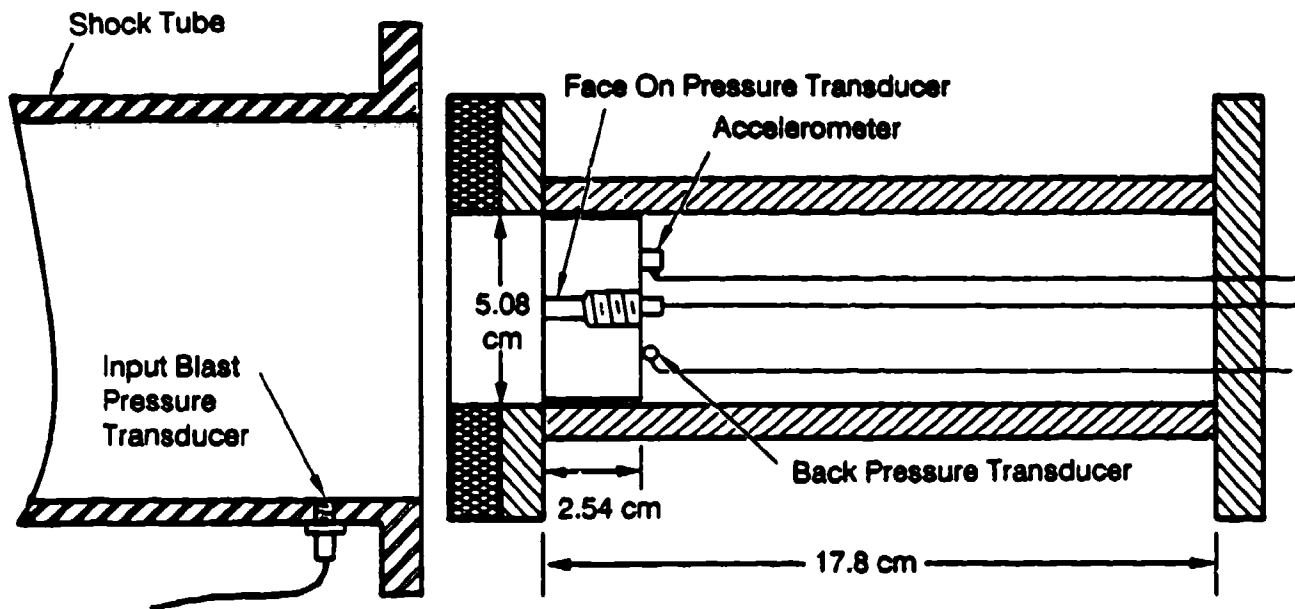


Figure 6. Schematic diagram of surrogate thorax model test setup.

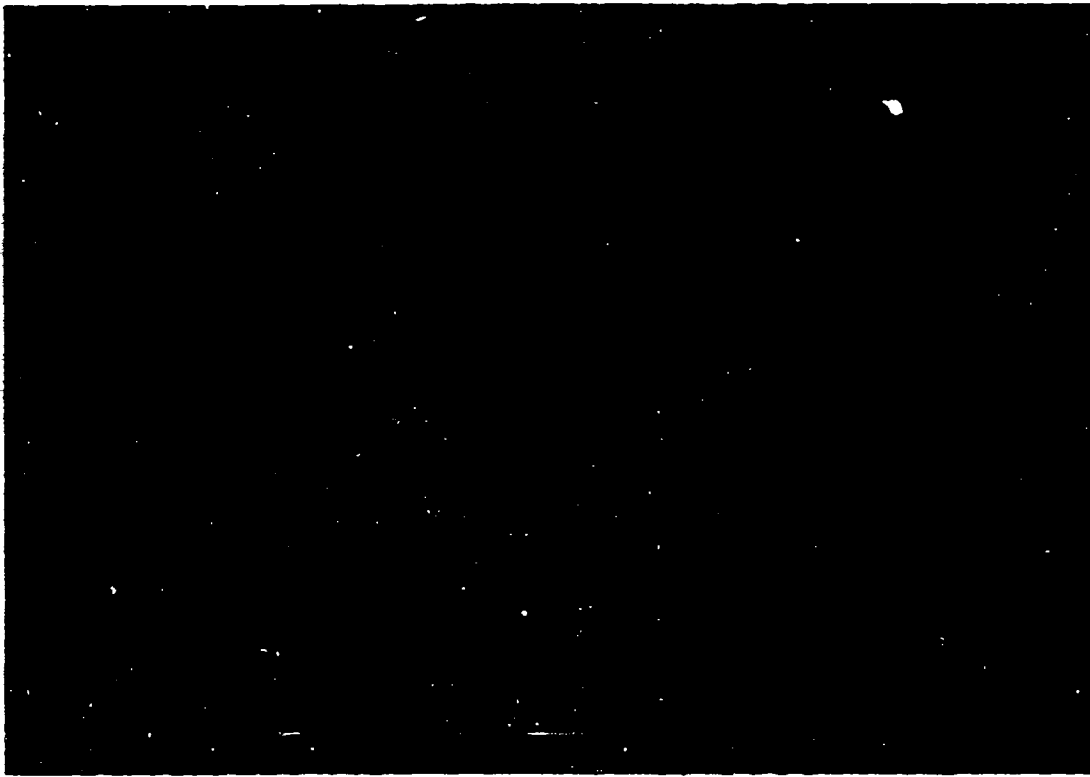


Figure 7. Surrogate thorax model test setup.

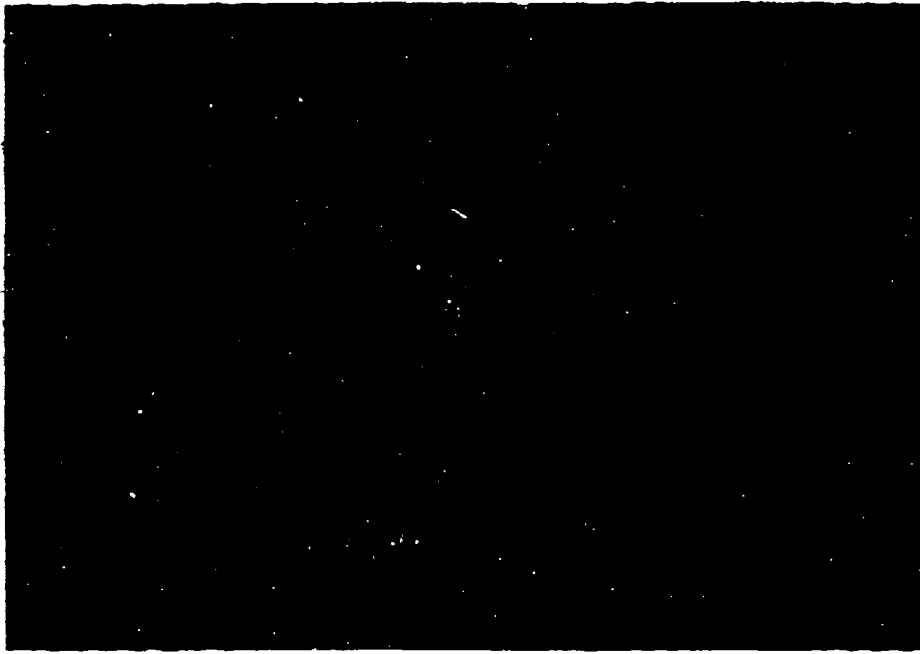


Figure 8. Chest wall model and instrumentation.

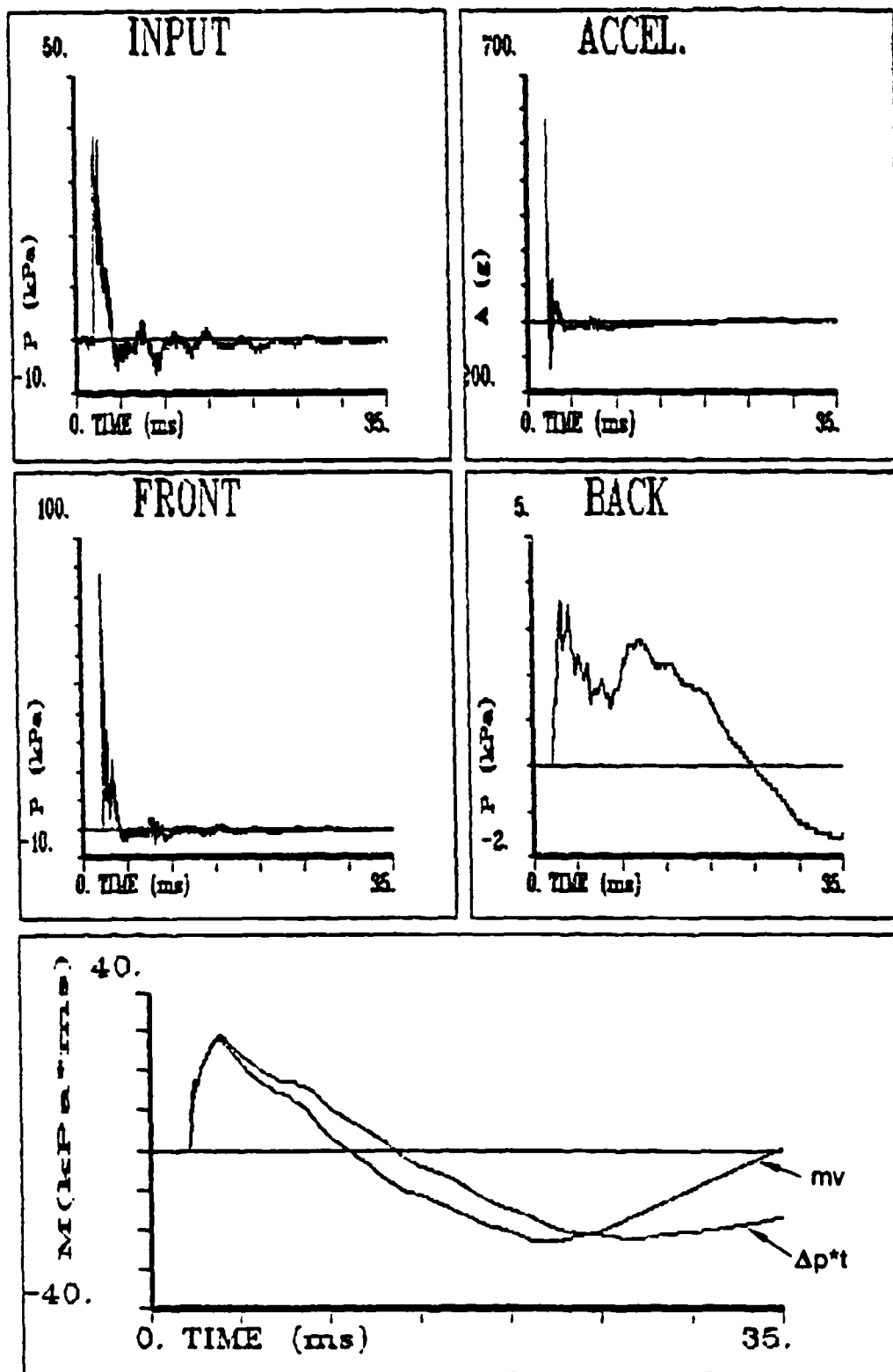


Figure 9. Loading measurements across a 1-D chest wall model. (FRONT, BACK and INPUT are pressure signals measured across the model and at the side wall; Δp^*t is the impulse and mv is the momentum.).

The comparison of these integrated quantities is shown in the bottom plot of Figure 9. The quantities are in close agreement during the acceleration phase of the loading, that is while the load exceeds the back pressure. During the deceleration phase, the momentum decreases faster than the impulse, although both reach the same minimum value. At the minimum momentum, the chest wall is moving *outward* at its maximum velocity. After this moment, the lung pleural pressure drops below ambient and the chest wall slows its outward motion. During this over-expansion phase, the momentum increases more rapidly than the impulse.

The agreement between these curves reflects the extent to which the model chest wall is free of forces other than those due to the front and back pressures. The discrepancies are probably not due to sliding friction since the velocity is slowed during the deceleration phase, but is increased during over-expansion. The differences at these later stages are of the order of the resolution of the pressure and acceleration instrumentation, whose scales have been set to capture the initial, large peaks. To within the experimental measurement error, therefore, we conclude that chest wall model is acted upon by only the blast loading and resulting pleural pressure.

4. APPLICATIONS OF THE SURROGATE MATERIAL AND THORAX MODEL

4.1 PRESSURE DISSIPATION IN THE SURROGATE MATERIAL

To determine the wave dissipation property of the foam, a 5.08 cm diameter, 1.5 m long Plexiglas pipe test fixture was fabricated. Pressure signals were measured along the wall at different distances from the neoprene membrane loading interface. Figure 10 shows typical outputs at various distances from the membrane. The nondimensionalized pressure is plotted in Figure 11. As shown, the pressure signal follows roughly an exponential decay in the region from the reference point (2.54 cm from the loading surface) to about 15 cm.

4.2 CORRELATION BETWEEN CHEST WALL VELOCITY AND PARENCHYMA PRESSURE

A correlation between the chest wall velocity and parenchyma pressure can be derived based on a work-energy relationship. Following Rouse (1946), the change in kinetic energy in a homogeneous material per unit volume, $\rho v^2/2$, must be equal to the work per unit volume, $\Delta p^2/2E$ done by the change in pressure, Δp . The work per unit volume is the product of average unit stress, $\Delta p/2$, and the resulting unit strain, $\Delta \rho/\rho = \Delta p/E$. Therefore,

$$\frac{\rho v^2}{2} = \frac{\Delta p}{2} \left(\frac{\Delta p}{E} \right) = \frac{\Delta p^2}{2E} \quad (4-1)$$

Hence, the pressure rise caused by the wave can be related to the chest wall velocity by

$$p = \sqrt{E\rho} \cdot v = \sqrt{E/\rho} \cdot \rho v = \rho c v \quad (4-2)$$

To test the validity of this relation for the thorax surrogate model, we use the data presented in Figure 9. Figure 12 compares the value of $\rho c v$ computed from the integral of the accelerometer and p taken from the foam-side transducer. Good agreement is obtained until the time that the reflected wave begins to act on the chest wall. The relation is expected to break down at this point, since the reflected wave is not the *result* of the chest wall motion.

A 5 cm diameter, 1 m long Plexiglas pipe was fabricated to accommodate the large displacement of the model chest wall and to eliminate the wave reflection effect. To deliver the large impulse, nail fasteners of the Powder-Actuated-Tool were used to impact directly on the target at close range. To prevent shock damage to the model, aluminum plate chest wall models

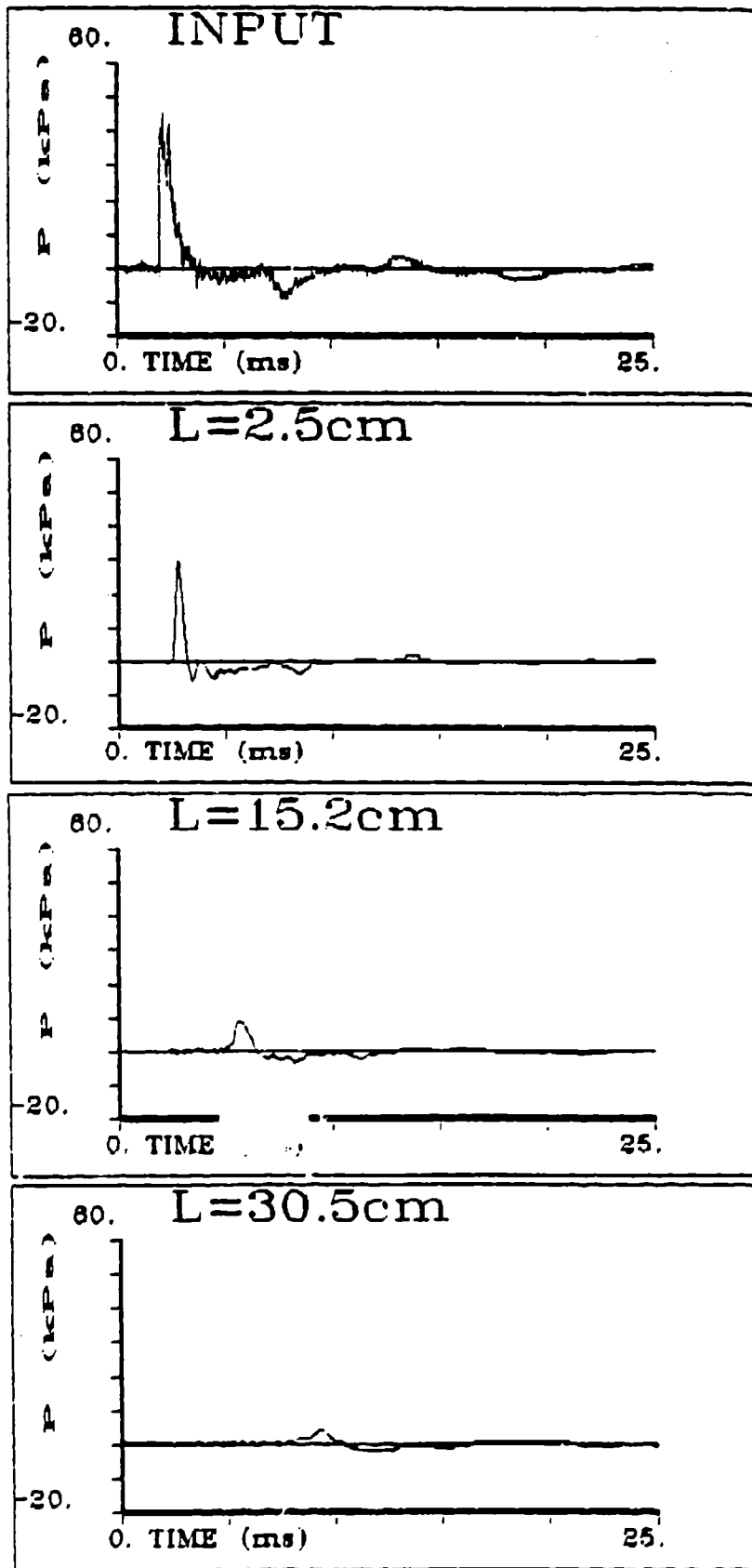


Figure 10. Blast pressure variation in the foam at various stations along the test pipe.

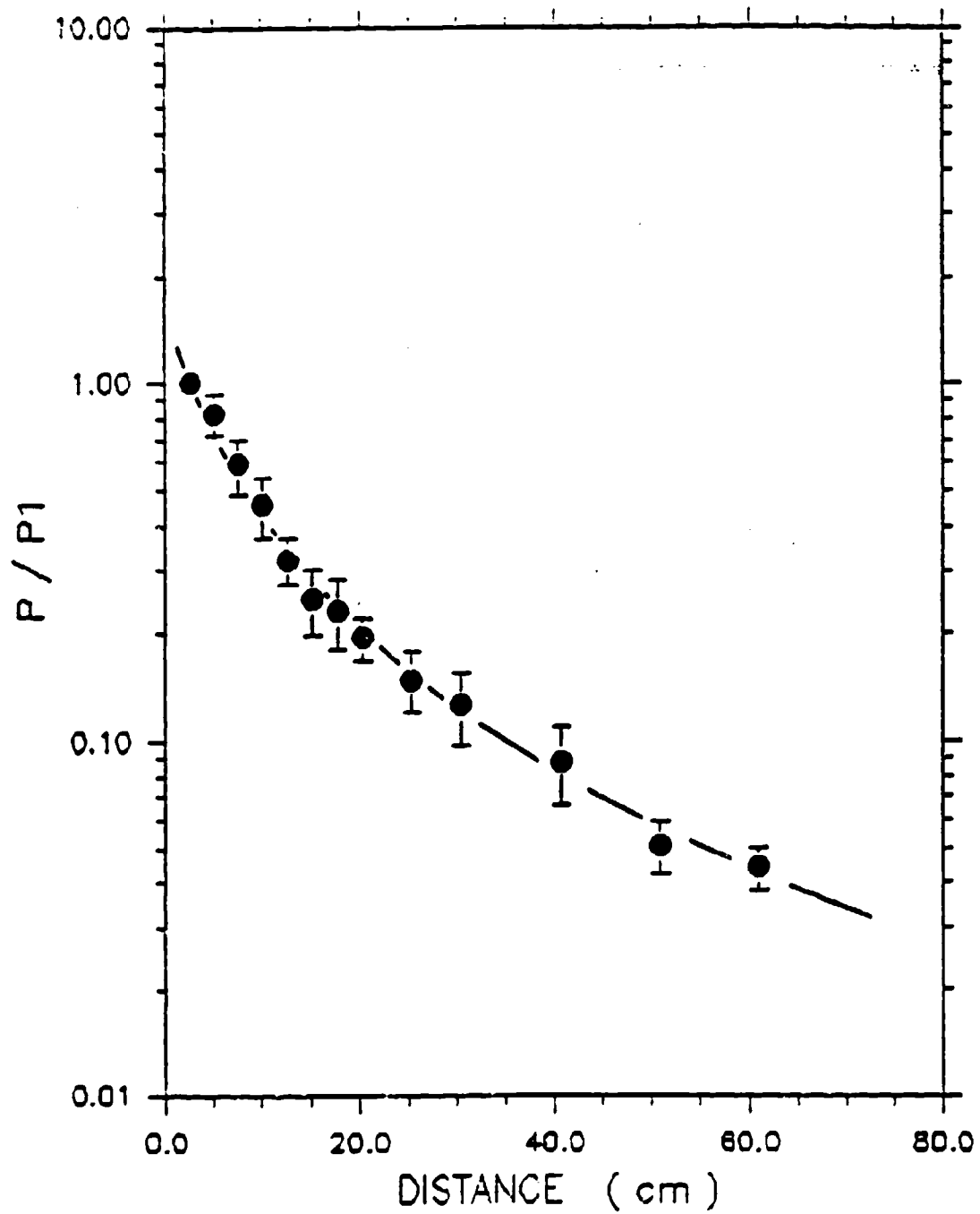


Figure 11. Pressure variation versus distance (p_1 is the pressure measured at 2.54 cm from loading interface).

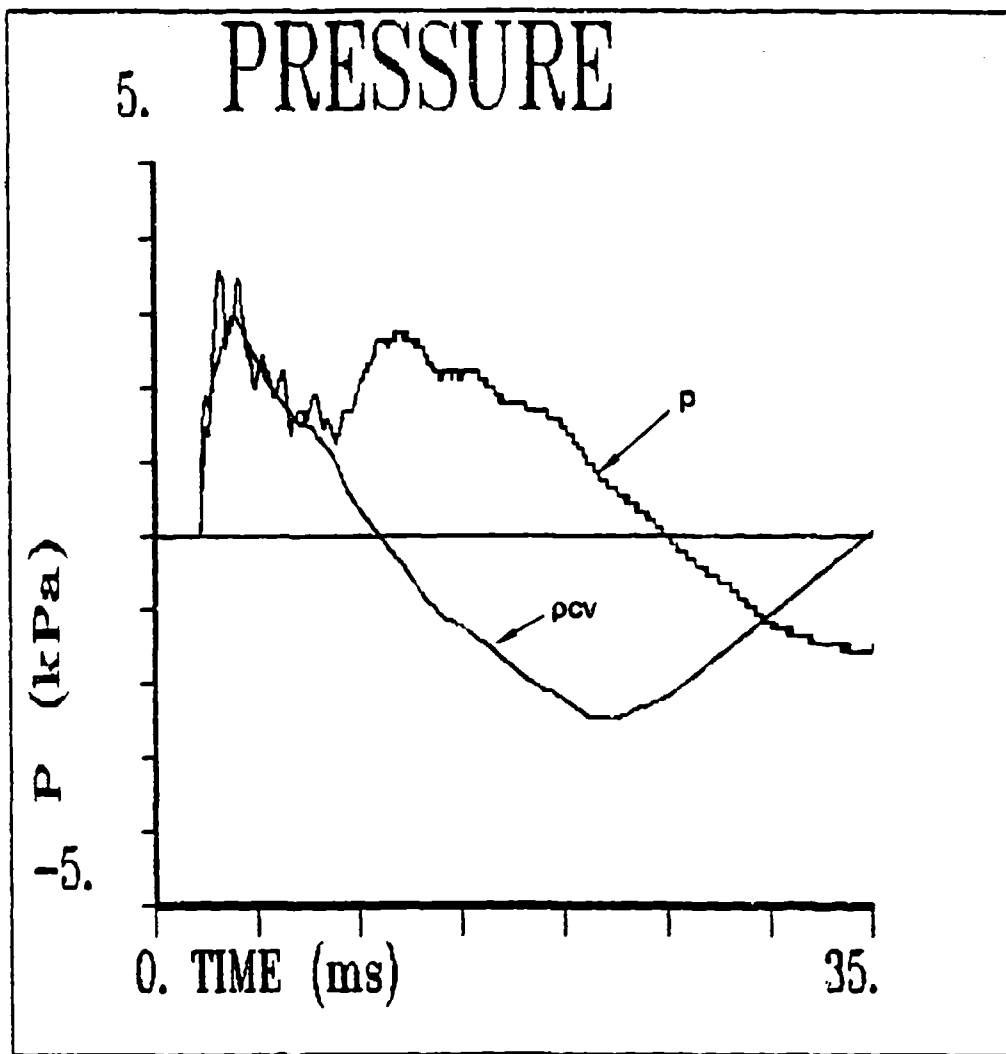


Figure 12. Comparison of the measurement results of p and pcv at the 1-D foam-chest wall model interface.

were used. Furthermore, a 1.2 cm thick hard rubber sheet was mounted in front of the model to increase the interaction time and to reduce the noise signal. Photographs of the high impulse chest wall model and the test pipe are shown in Figure 13(a) and (b).

To measure the velocities associated with the high impulse, a 50,000 g PCB Model 305A accelerometer was acquired. This accelerometer can be used to measure a velocity rise of up to 50 m/s in 0.1 ms.

During the impact, the surrogate material behind the chest wall model was subjected to a high compression loading followed by a recoil motion. This process tends to produce large voids in the foam that destroys its uniformity and creates questionable test results. To alleviate this problem, the surrogate material in the affected region was discarded and replaced with new material after each shot.

To prevent impact damage to the forward facing pressure transducer, only the acceleration and back pressure at the interface between the target and foam were measured to test the $p = \rho cv$ relationship. Furthermore, in order to reduce the acceleration-induced pressure signal, a relatively acceleration-insensitive strain-gauge-type Entran pressure transducer was used. Figure 14(a) and (b) shows two sets of measurements of pressure, acceleration, and velocity. As shown, up to the test velocity of 11 m/s, the results of ρcv agree well with P , similar to that for small amplitude waves. In other words, no special features that might be related to finite amplitude wave effects are revealed.

Beyond the peak pressure, ρcv deviates from the measured pressure signal. This is mainly caused by the large acceleration range measured by the accelerometer. The small acceleration in the negative phase is comparable to the instrumentation resolution and can not be measured accurately. Consequently, integration results vary randomly. The irregular pressure spikes shown in Figure 14(b) could be the result of sensor fatigue or damage caused by the intense shock loading.

4.3 INTERPRETATION OF INTRATHORACIC PRESSURE (ITP) MEASUREMENT

Presently, reference lung pressures are obtained from pressure transducers placed either in the esophagus or in the bronchial tubes. Depending on the probe size and depth of insertion, the pressure transducer might trap air ahead of it or be enclosed by air. In either case, the transducer measures the pressure in an air-filled region which may not be the same as that of the lung parenchyma.

To address this issue, the following demonstrative tests were carried out. Figure 15 shows the test setup schematic for these pressure measurements. First, the pressure signal in a slender air-filled balloon (0.60 cm diameter, 3.18 cm long) was compared with that obtained directly from the foam. As shown in Figure 16, the pressure in the foam has the typical sharp pressure rise, whereas that inside the balloon has a more gradual pressure rise.

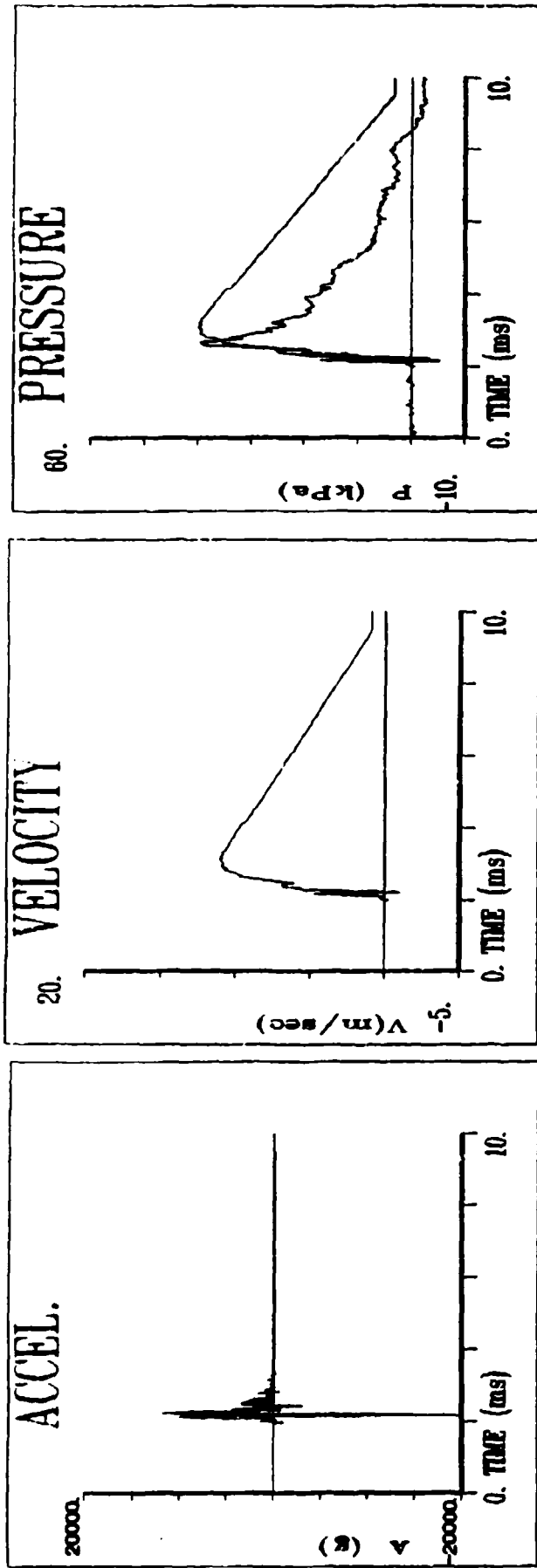
The tests were repeated using a foam-filled balloon. As shown in Figure 17, despite part of the load being carried by the balloon, and hence a slight reduction in amplitude, the signal inside the balloon has essentially the same sharp pressure rise as that outside.



Figure 13a. High impulse chest wall model.

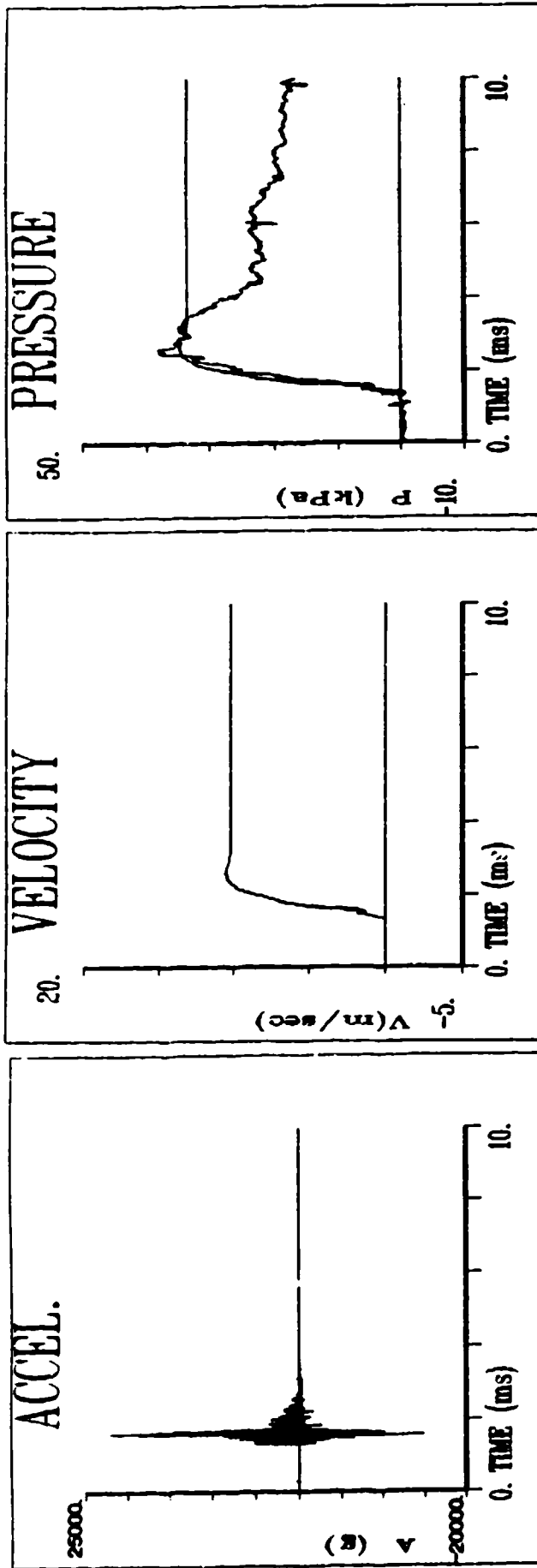


Figure 13b. High impulse chest wall test model setup.



(a)

Figure 14. Comparison of p vs. pcv for high impulse model test.



(b)

Figure 14. (Cont'd).

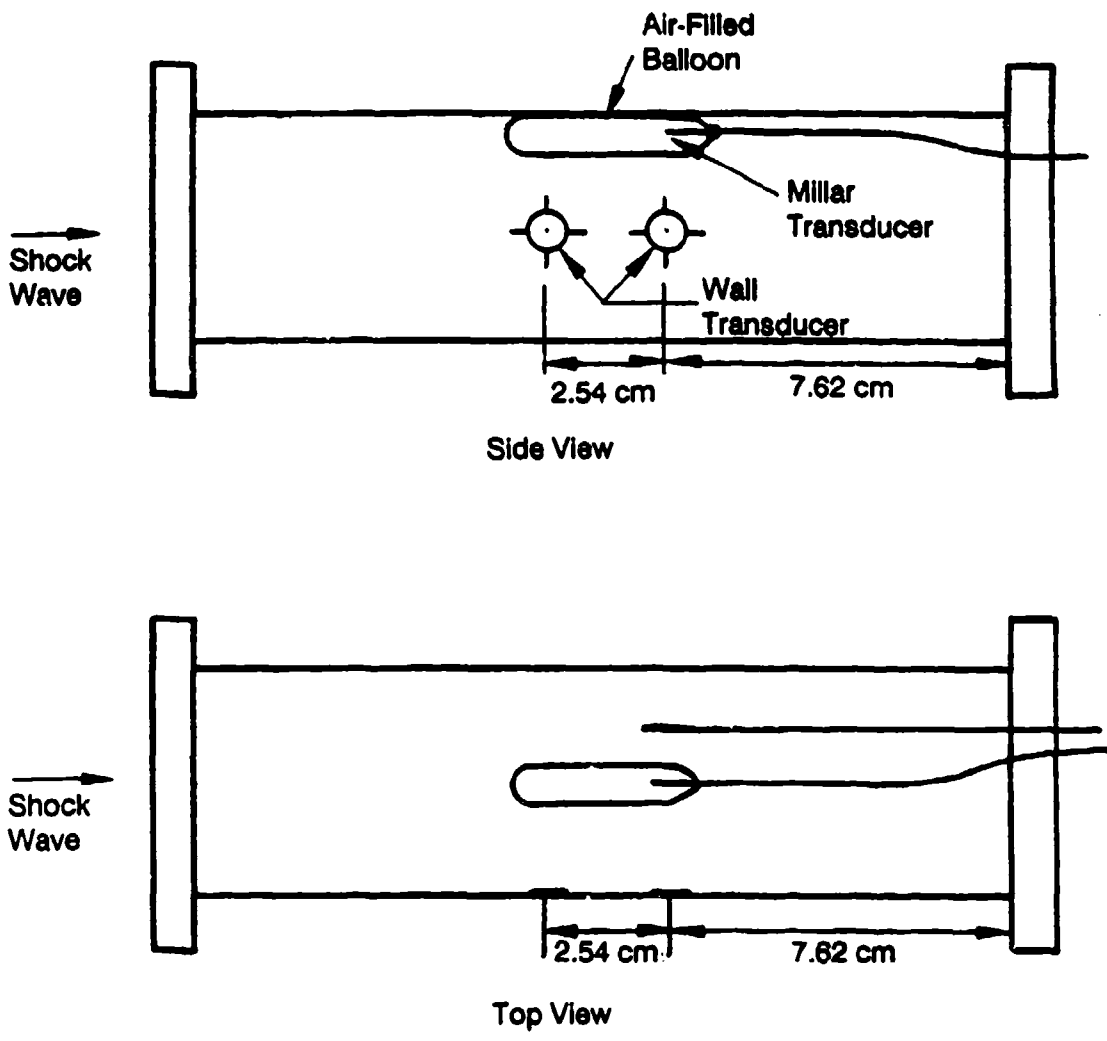
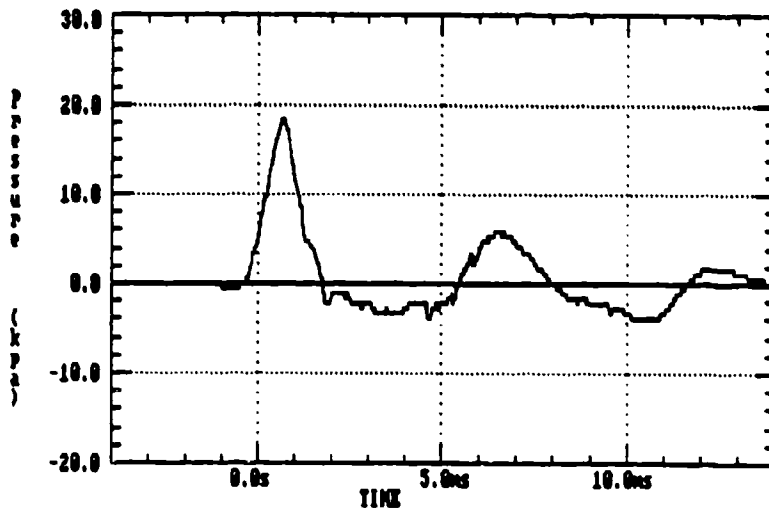
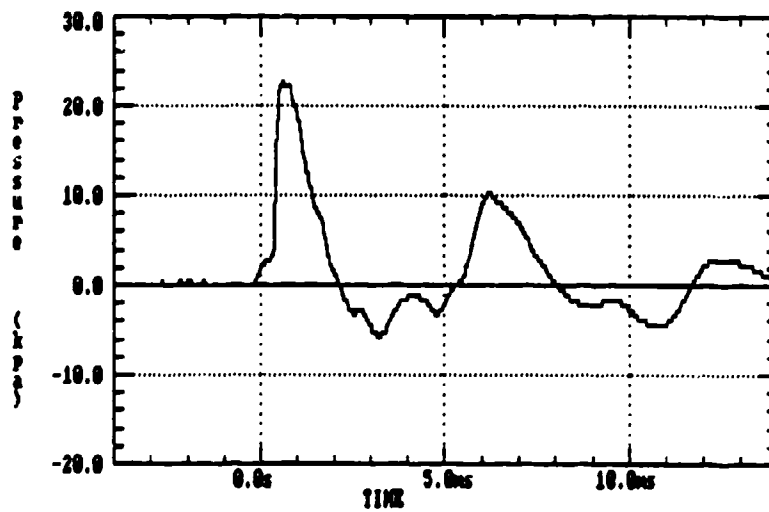


Figure 15. Test setup for pressure measurements in air sack vs. in surrogate lung material.

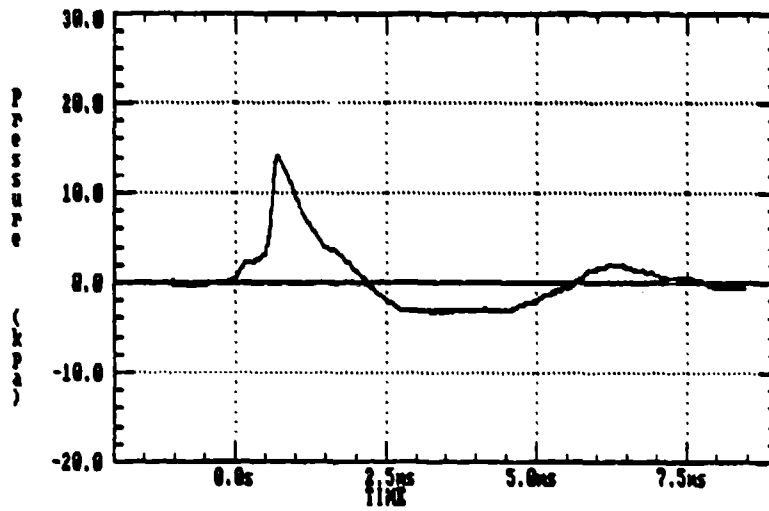


(a) Pressure signal inside air-filled balloon

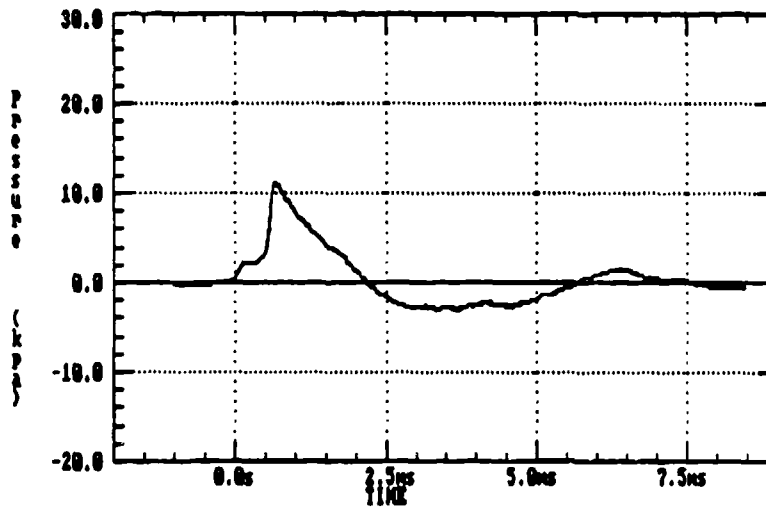


(b) Pressure in surrounding foam

Figure 16. Pressure signal inside vs. outside of a tubular balloon.



(a) Pressure signal inside air-filled balloon



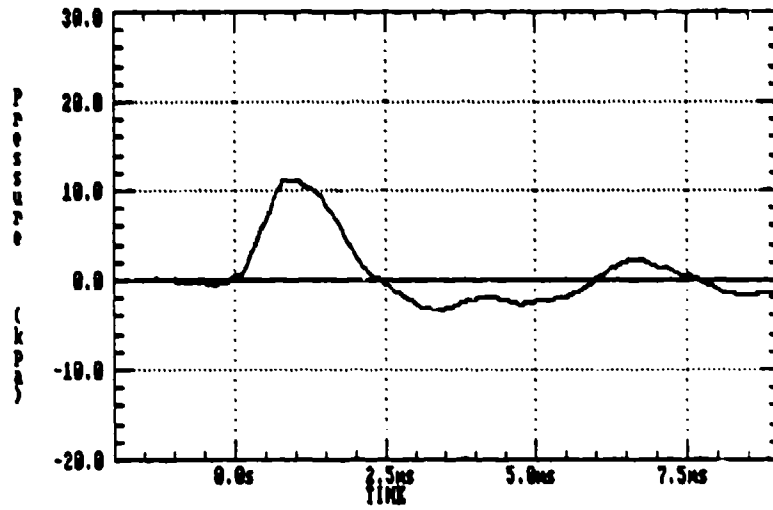
(b) Pressure in surrounding foam

Figure 17. Pressure signals inside a foam-filled balloon and in the surrounding foam.

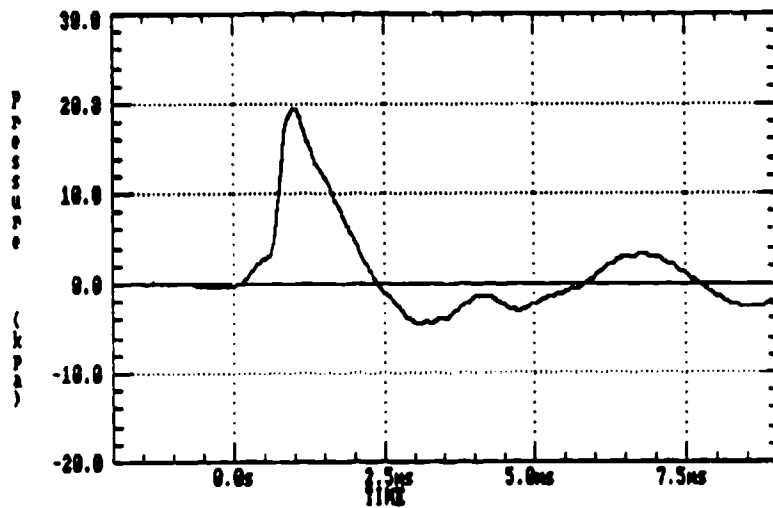
A third test compares the signals from two balloons, one filled with foam and one filled with air. As shown in Figure 18, the results show patterns similar to the pair shown in Figure 16, namely, the one filled with foam has a steeper pressure rise than the one filled with air.

In a final test, an isolated rabbit lung lobe was placed in the foam-filled test chamber and subjected to blast impulse as before. The pressure signals obtained from a bronchial tube, lung parenchyma, and foam are compared. As shown in Figure 19, the signal in the foam agrees well with that in the lung parenchyma, while the signal obtained in the air-filled bronchial tube differs from both signals and is characterized by a smooth pressure rise.

These results illustrate that the pressure signals measured in an air-filled cavity tend to have a smooth rise, whereas those measured directly in the two-phase medium tend to be shock-like, with a steep rise and a larger amplitude. This finding implies that conventional ITP measurements obtained inside a bronchial tube or the esophagus could differ significantly from the true parenchyma pressure. Furthermore, since the rigidity and dimension of bronchial tubes vary from generation to generation, they may produce different ITP signals. Carefully controlled field tests to compare the parenchyma pressure with those measured at various generations of the bronchial tubes are recommended to quantify this relationship.

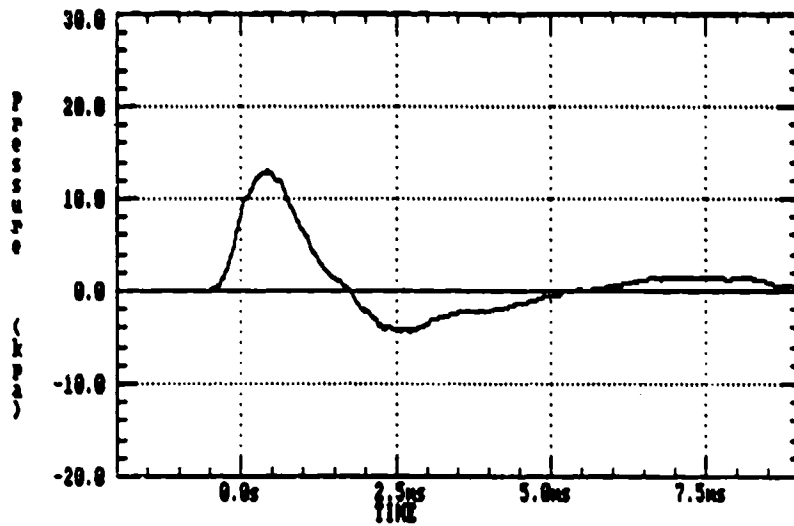


(a) Air-filled balloon

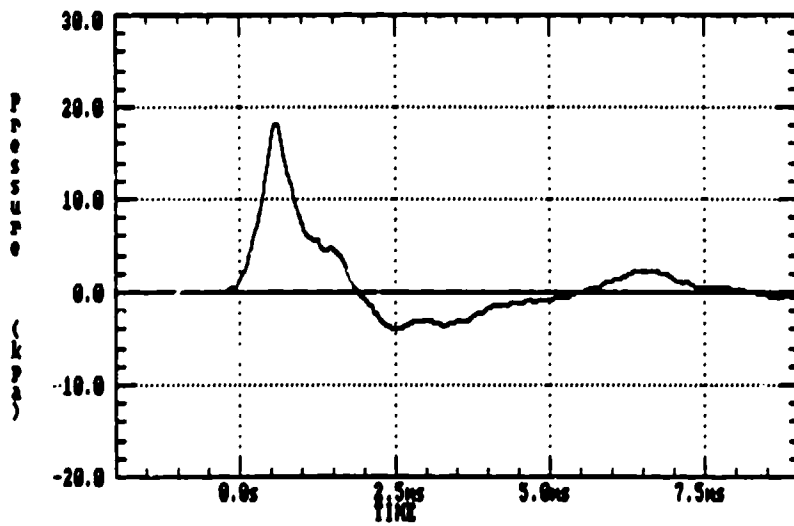


(b) Foam-filled balloon

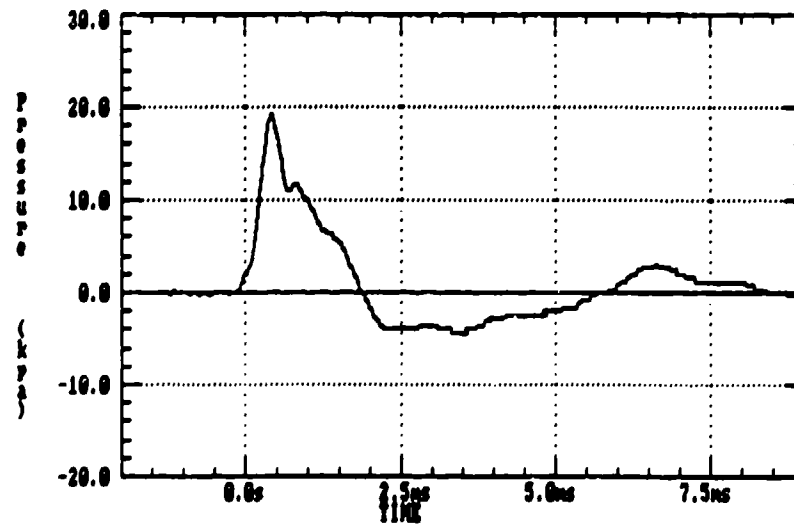
Figure 18. Pressure signal inside an air-filled balloon vs. a foam-filled balloon



(a) Bronchial pressure



(b) Parenchymal pressure



(c) Surrounding foam pressure

Figure 19. Pressure signals in the bronchi, parenchyma, and surrogate lung material. (Initial airway pressure = 10 cm H₂O. Pleural pressure = pressure of surrogate material = atmospheric pressure = 0 cm H₂O.)

5. CONCLUSIONS

A surrogate material was sought to facilitate laboratory model tests on the dynamics of blast injury of the lung. Off-the-shelf shaving cream (foam) was found to have a nominal density of 0.1 g/cm^3 and a wave speed of 35 m/s, similar to that of the lung parenchyma, and was chosen as the surrogate material.

Pressure measurements in a foam-filled tube indicate that a shock-like pressure wave develops in the foam under blast loading. This wave is dissipated and dispersed as it moves downstream.

The shock-like characteristics are absent, however, when the pressure is measured in a small-diameter tubular balloon, or in the bronchial tube of a rabbit lung, placed in the foam. This result suggests that conventional intrathoracic pressure (ITP) measurements obtained in animal airways or the esophagus may not be representative of the true lung parenchymal pressure and could be misleading.

A thoracic model that uses the surrogate lung material and a chest wall model was fabricated to test the applicability of the $p = \rho cv$ relationship. It was found that within the blast loading range tested, which produces accelerations of up to about 20,000 g and velocities of 11 m/sec, pressure signals up to their peaks agree well with ρcv . Limitations in instrument resolution, however, preclude the comparison beyond peak pressure.

REFERENCES

- Agostoni, E., E. D'Angelo, and M. V. Bonanni, "Topography of Pleural Surface Pressure Above Resting Volume in Relaxed Animals," *J. Appl. Physiol.*, Vol. 29(5): 297-306 (1970).
- Campbell, I. J. and A. S. Pitcher, "Shock Wave in a Liquid Containing Gas Bubbles," *Proc. Roy. Soc. (London), Ser. A*, 243: 534-545 (1958).
- Fung, Y. C., M. R. Yen, and Y. J. Zeng, "Characterization and Modeling of Thoraco-Abdominal Response to Blast Waves, Vol. 3. Lung Dynamics and Mechanical Properties Determination," JAYCOR Final Report to WRAIR, 1985.
- Proctor, D. F., P. Caldini, and S. Permutt, "The Pressure Surrounding the Lungs," *Respir. Physiol.* 5: 130-144 (1968).
- Rice, D. A., "Sound Speed in Pulmonary Parenchyma," *J. Appl. Physiol.: Respir. Envir. Exercise Physiol.* 54(1): 304-308 (1983).
- Richmond, D. R., E. G. Damon, E. R. Fletcher, I. G. Bowen, C. S. White, "The Relationship Between Selected Blast-Wave Parameters and the Response of Mammals Exposed to Air Blast," *Ann. N. Y. Acad. Sci.*, Vol. 152, Article 1, 103-121 (1968).
- Rouse, H., Elementary Mechanics of Fluids, John Wiley & Sons, Inc., New York, 1946.
- Selkurt, E. E., Physiology, Little, Brown and Co., Boston, 1976.
- Yen, M. R., Y. C. Fung, H. H. Ho, and G. Butterman, "Speed of Stress Wave Propagation in the Lung," *J. Appl. Physiol.*, 61(2), 701-705 (1986).
- Yu, J. H.-Y., E. J. Vassel, and C. J. Chuong, "Characterization and Modeling of Thoraco-Abdominal Response to Blast Waves, Vol. 8. Effect of Clothing on Thoracic Response," JAYCOR Final Report to WRAIR, 1985.

DISTRIBUTION LIST

4 copies **Director**
Walter Reed Army Institute of Research
ATTN: SGRD-UWZ-C
Washington, DC 20307-5100

1 copy **Commander**
US Army Medical Research and Development Command
ATTN: SGRD-RMI-S
Fort Detrick, Frederick, MD 21701-5012

2 copies **Defense Technical Information Center (DTIC)**
ATTN: DTIC-DDAC
Cameron Station
Alexandria, VA 22304-6145

1 copy **Dean**
School of Medicine
Uniformed Services University of the Health Sciences
4301 Jones Bridge Road
Bethesda, MD 20814-4799

1 copy **Commandant**
Academy of Health Sciences, US Army
ATTN: AHS-CDM
Fort Sam Houston, TX 78234-6100